Am J Physiol Lung Cell Mol Physiol 308: L797–L806, 2015.
First published February 6, 2015; doi:10.1152/ajplung.00276.2014.

Neonatal hyperoxic lung injury favorably alters adult right ventricular remodeling response to chronic hypoxia exposure

Kara N. Goss,[1] Anthony R. Cucci,[1] Amanda J. Fisher,[2] Marjorie Albrecht,[1] Andrea Frump,[1] Roziya Tursunova,[1] Yong Gao,[3] Mary Beth Brown,[4] Irina Petrache,[1,5] Robert S. Tepper,[3] Shawn K. Ahlfeld,[3]* and Tim Lahm*[1,5]

[1]*Division of Pulmonary, Allergy, Critical Care and Occupational Medicine, Indiana University School of Medicine, Indianapolis, Indiana;* [2]*Department of Anesthesiology, Indiana University School of Medicine, Indianapolis, Indiana;* [3]*Department of Pediatrics, Indiana University School of Medicine, Indianapolis, Indiana;* [4]*Department of Physical Therapy, School of Health and Rehabilitation Sciences, Indiana University School of Medicine, Indianapolis, Indiana;* [5]*Richard L. Roudebush VA Medical Center, Indianapolis, Indiana*

Submitted 26 September 2014; accepted in final form 6 February 2015

Goss KN, Cucci AR, Fisher AJ, Albrecht M, Frump A, Tursunova R, Gao Y, Brown MB, Petrache I, Tepper RS, Ahlfeld SK, Lahm T. Neonatal hyperoxic lung injury favorably alters adult right ventricular remodeling response to chronic hypoxia exposure. *Am J Physiol Lung Cell Mol Physiol* 308: L797–L806, 2015. First published February 6, 2015; doi:10.1152/ajplung.00276.2014.—The development of pulmonary hypertension (PH) requires multiple pulmonary vascular insults, yet the role of early oxygen therapy as an initial pulmonary vascular insult remains poorly defined. Here, we employ a two-hit model of PH, utilizing postnatal hyperoxia followed by adult hypoxia exposure, to evaluate the role of early hyperoxic lung injury in the development of later PH. Sprague-Dawley pups were exposed to 90% oxygen during postnatal *days 0–4* or *0–10* or to room air. All pups were then allowed to mature in room air. At 10 wk of age, a subset of rats from each group was exposed to 2 wk of hypoxia (P_{atm} = 362 mmHg). Physiological, structural, and biochemical endpoints were assessed at 12 wk. Prolonged (10 days) postnatal hyperoxia was independently associated with elevated right ventricular (RV) systolic pressure, which worsened after hypoxia exposure later in life. These findings were only partially explained by decreases in lung microvascular density. Surprisingly, postnatal hyperoxia resulted in robust RV hypertrophy and more preserved RV function and exercise capacity following adult hypoxia compared with nonhyperoxic rats. Biochemically, RVs from animals exposed to postnatal hyperoxia and adult hypoxia demonstrated increased capillarization and a switch to a fetal gene pattern, suggesting an RV more adept to handle adult hypoxia following postnatal hyperoxia exposure. We concluded that, despite negative impacts on pulmonary artery pressures, postnatal hyperoxia exposure may render a more adaptive RV phenotype to tolerate late pulmonary vascular insults.

prematurity; right ventricular adaptation; pulmonary hypertension; capillarization; atrial natriuretic peptide

PULMONARY ARTERIAL HYPERTENSION (PAH) is a devastating and progressive pulmonary vasculopathy affecting all ages, ultimately leading to right ventricular (RV) failure and death (14). Although the etiology of PAH is multifactorial and incompletely understood, the disease is considered to be the consequence of a "two-hit" phenomenon, suggesting that multiple factors must align for its development (43). Although influences such as genetic predisposition or hormonal abnormalities have been identified as first hits, the potential contribution from early abnormal alveolar and vascular development has not been fully evaluated (4, 11).

A recent NHLBI Workshop on the Primary Prevention of Chronic Lung Diseases identified a need to study "at-risk" subjects for the development of PAH (5, 17). Along these lines, a better understanding of early-life risk factors for development of PAH is needed. Normally, the perinatal window represents a critical time of lung development, where infants must transition from the simple saccular phase, with rapid expansion of the distal airspaces to the mature alveolar phase, with bulk alveolarization continuing into early childhood (20). Contemporary advancements in perinatal and neonatal care have lowered the limit of viability to ~23 wk of gestation. Preterm infants born before 28 wk of gestation have an immature saccular lung that frequently is injured by exposure to life-saving mechanical ventilation and a significant amount of supplemental oxygen. Such noxious exposures disrupt normal lung development and, as a result, the majority of extremely preterm infants develop chronic lung disease (47). In its most severe form, premature chronic lung disease manifests as bronchopulmonary dysplasia (BPD), a disease characterized primarily by impaired alveolar septation and decreased pulmonary vascular density (10, 13, 24, 26, 52, 54). Despite continually improving ventilation strategies in the newborn period, the increased survival of extremely preterm infants has increased the burden of BPD (18, 49). This vast number of premature infants continues to represent a group at risk for pulmonary alveolar and vascular disease. In fact, prematurity serves as an independent risk factor for the development of neonatal pulmonary hypertension (PH), with roughly one in six extremely preterm infants affected (9).

Evidence exists that arrested lung development attributable to postnatal hyperoxia exposure, as is frequently seen with prematurity, also affects the pulmonary vasculature later in life. For example, in animal models, even brief exposure of the developing lung to hyperoxia is associated with impaired alveolarization and decreased pulmonary arterial density that persist into adulthood (3, 15, 35, 56, 57). This is thought to be attributable to subtle yet significant direct effects on the pulmonary vasculature, suggesting that the pulmonary vascular compartment is exquisitely sensitive to even brief insults during development. Postnatal hyperoxia exposure and lung injury also represent risk factors for later pulmonary vascular and RV abnormalities in humans (31, 41). Although these studies

* S. Ahlfeld and T. Lahm contributed equally to this work.
Address for reprint requests and other correspondence: T. Lahm, Indiana Univ. School of Medicine, Joseph E. Walther Hall, Rm. C 400, 980 W. Walnut St., Indianapolis, IN 46202 (e-mail: tlahm@iu.edu).

suggest that postnatal hyperoxia exposure may represent a risk factor for the development of PH later in life, no controlled experimental studies have been performed that evaluate whether and how postnatal hyperoxia affects the pulmonary vasculature and RV upon exposure to a second insult later in life.

Here, we utilize a novel two-hit model of PH to identify the role of postnatal hyperoxic lung injury in independently and synergistically promoting PH development later in life. Specifically, we investigated whether postnatal hyperoxia exposure of the developing saccular lung predisposes rats to the development of PH in adulthood following another common pulmonary vascular insult, chronic hypoxia exposure. Hypoxia was selected as a second hit because the high prevalence of chronic lung diseases and sleep-disordered breathing in the Western world would suggest that many prematurely born individuals will be exposed to a relevant degree of hypoxia later in life (7, 46, 53). We employed a comprehensive experimental model to investigate the mechanisms by which varying severities of early hyperoxic lung injury alter later responses to hypoxia. We found that early hyperoxia exposure indeed worsens pulmonary hypertensive responses later in life. However, despite a more severe PH phenotype in this population, the degree of RV adaptation to the increased afterload was more preserved in animals undergoing early hyperoxia exposure. We propose that early hyperoxia exposure allows for development of adaptive mechanisms in the RV, thus contributing to an improved tolerance of pulmonary vascular insults such as hypoxia later in life.

MATERIALS AND METHODS

Animal models. Timed pregnant Sprague-Dawley dams (Harlan, Indianapolis, IN) were allowed to deliver naturally at term in house. Within 12 h of birth, male and female newborn rat pups were pooled and randomized into one of three groups: *1*) room air (RA), *2*) 4-day hyperoxia ($4dO_2$), or *3*) 10-day hyperoxia ($10dO_2$; see Fig. 1 for timeline). The two durations of hyperoxia exposure were used to determine a dose response to postnatal hyperoxia, thus mimicking a mild and a moderate-to-severe hyperoxic lung injury. The hyperoxia groups were housed in standard cages within a 30" × 20" × 20" polypropylene chamber with a clear acrylic door (BioSpherix, Lacona, NY), as previously described (3). Oxygen concentration within the chamber was maintained at or above a fraction of inspired oxygen ($F_{I_{O_2}}$) of 0.9 using of a continuous oxygen sensor. Dams were rotated between RA and hyperoxia every 24–48 h to prevent oxygen toxicity. For hyperoxia-exposed pups, dams and pups were removed from the hyperoxia chamber after 4 or 10 days, respectively, and returned to RA. All pups were then allowed to mature with their respective dams and were weaned at 3 wk of age. At 10 wk of age, half of the rats from each group were exposed to hypobaric hypoxia (P_{atm} = 362 mmHg; equivalent to $F_{I_{O_2}}$ of 0.1 at sea level) in a custom-made hypobaric hypoxia chamber for an additional 2 wk as previously described (29). Before initiation and after completion of 2 wk of hypoxia exposure, a

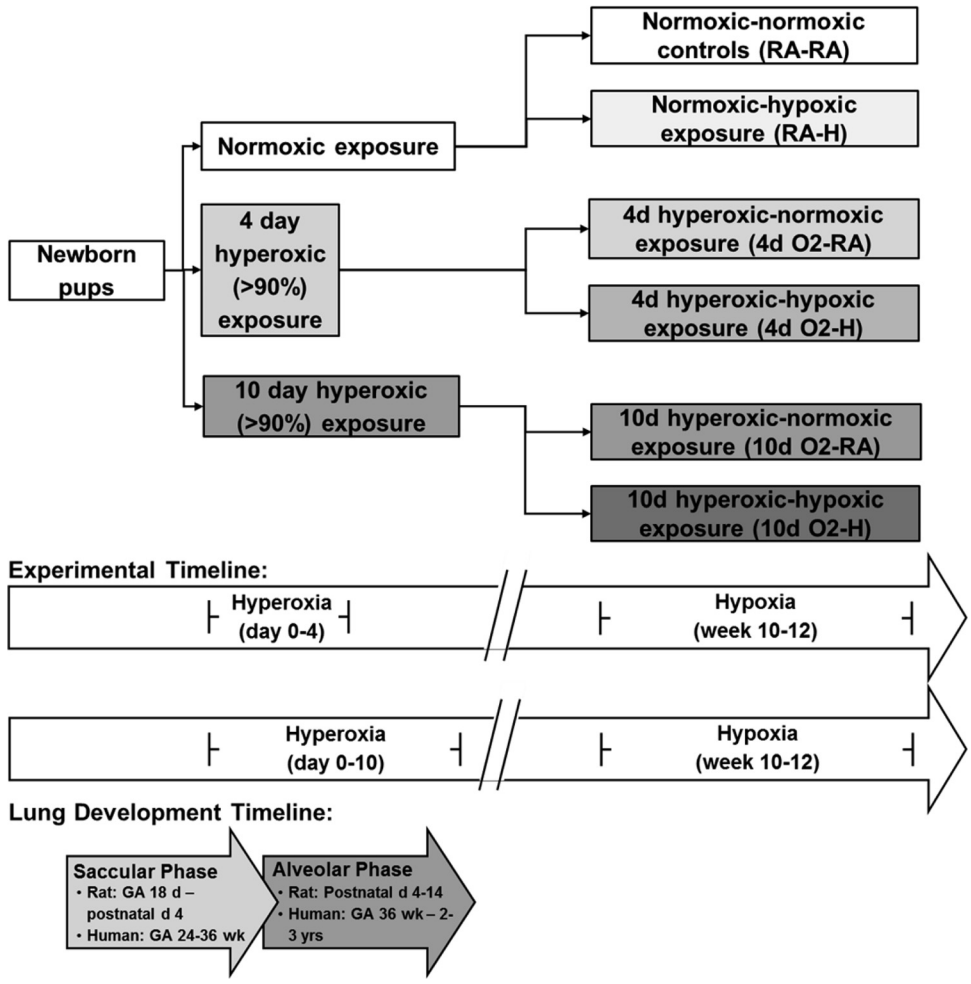

Fig. 1. Timeline of experimental exposures. Brief hyperoxia (4-day, 4d) exposure is limited to the period of saccular lung development, whereas prolonged hyperoxia (10-day, 10d) exposure includes injury well into the bulk alveolarization phase. RA, room air; H, hypoxia; GA, gestational age.

subset of animals underwent exercise testing for determination of maximal oxygen consumption ($\dot{V}O_{2\,max}$; see below). At the end of the 2-wk hypoxia exposure, animals underwent echocardiography, hemodynamic assessments, and death. Animals were allowed access to food and water ad libitum. All animal protocols were approved by the Indiana University Institutional Animal Care and Use Committee.

Exercise testing. A subset of animals (n = 6–7/group) began treadmill familiarization at 8 wk of age, consisting of running 5 min per day, 4 times per week for 2 wk at progressively faster pace (6–20 m/min) and incline (0–20°). This workload was selected to promote familiarization to the treadmill without promoting a training effect (30). At 10 and 12 wk of age (before the start and after the completion of the 2-wk hypoxia exposure), animals performed exercise testing for maximal oxygen consumption ($\dot{V}O_{2\,max}$). Metabolic measurements were obtained using an indirect open-circuit calorimetric system (Oxymax; Columbus Instruments, Columbus, OH). A gas analyzer was calibrated using standardized gas mixtures (Praxair, Danbury, CT), and baseline measurements were collected until $\dot{V}O_2$ consumption stabilized. A graded exercise test was performed, consisting of a stepwise increase in treadmill speed and incline stages every 3 min as follows: Stage I 10 m/min at 0°, Stage II 10 m/min at 5°, followed by an increase by 5 m/min and 5° for each consecutive stage. The test was terminated when $\dot{V}O_2$ plateaued despite increasing workload or if the rat was unable to maintain position on the treadmill belt despite three consecutive shocks without recovery (8). All $\dot{V}O_{2\,max}$ values are expressed relative to body weight, and the highest achieved $\dot{V}O_2$ was recorded as the $\dot{V}O_{2\,max}$. To avoid acute effects of exercise testing on echocardiographic, hemodynamic, and biochemical endpoints, at least 2 days were allowed between exercise testing and further assessments.

Echocardiography. Rats were lightly anesthetized with 1–2% isoflurane via nosecone to achieve adequate anesthesia with a heart rate (HR) of 300–400 beats/min. Two-dimensional short-axis and long-axis images were acquired using a high-resolution ultrasound system (Vevo 2100; VisualSonics, Toronto, Ontario, Canada) equipped with an 18–38-MHz scan probe. Long axis was used to measure the RV outflow tract (RVOT) at the level of the tricuspid valve at mid systole. Doppler was used to identify maximal velocities within the pulmonary artery (PA) and record velocity time interval (VTI; calculated with Vevo Analysis software on 3 consecutive cardiac cycles). Stroke volume (SV) was determined using the formula $SV = VTI \times 3.142 \times (½RVOT)^2$, with cardiac output (CO) calculated by $CO = SV \times HR$. In a subset of animals, we assessed RV fractional shortening, measured by the change in end-diastolic to end-systolic diameter divided by the end-diastolic diameter [(EDD − ESD)/EDD], as a measure of cardiac contractility and performance (32). Rats were recovered from anesthesia after determination of all echocardiographic endpoints.

Hemodynamic measurements. After a recovery period of at least 4 h following echocardiography, rats were anesthetized with isoflurane (1–2%) and orally intubated. The left carotid artery and right internal jugular vein were cannulated, and a 2F Millar catheter (Model SPR-513; Millar Instruments, Houston, TX) was advanced into the RV as previously described (29). RV systolic pressure (RVSP) and mean arterial pressure (MAP) were recorded on 2% isoflurane with supplemental oxygen, after verification of euthermia, normocapnea, and normal pH. Once all hemodynamic endpoints were obtained, animals were euthanized by exsanguination under anesthesia via the arterial line, followed by immediate organ harvest.

RV hypertrophy. RV hypertrophy (RVH) was assessed by measuring the Fulton index [weight of RV divided by weight of the left ventricle plus septum; RV/(LV + S)]. Immediately after determination of RV and LV + S weights, the apex was placed in formalin for later determination of capillarization; the rest of the RV was snap-frozen for further biochemical analyses.

Pulmonary vascular remodeling. Lungs were flushed with normal saline through a catheter inserted into the PA until clear return was obtained from the left atrium. After excision of the right lung, the left lung was then inflated via the trachea with 10% buffered formalin in agarose under constant pressure (15 mmHg), removed from the thoracic cavity, and embedded in paraffin. Verhoeff-Van Gieson immunohistochemical staining was performed on lung sections, as previously described (39). Pulmonary vascular wall area was then determined in a blinded fashion by tracking the inner and outer border of small- and medium-sized PAs (<200 μm diameter, 10 vessels per animal, ×20 objective) using Kodak software and by dividing the measured area (pulmonary wall area) by the entire vessel area (entire area encompassed by outer pulmonary arterial wall border, representing pulmonary wall area + lumen area). Pulmonary vascular remodeling was expressed as the ratio of the pulmonary wall area to the entire vessel area. PAs were identified by proximity to terminal bronchioles or alveolar ducts, as described previously (29). Images were obtained using a Nikon Eclipse 80i microscope with camera and NIS-Elements AR 3.0 software (Nikon Instruments, Melville, NY).

For pulmonary microvascular density, immunohistochemical staining with von Willebrand Factor [vWF; rabbit polyclonal anti-human vWF (A0082), 1:2,500; Dako, Carpenteria, CA] was performed utilizing the Vectastain Elite ABC kit (Vector Laboratories, Burlingame, CA) with diaminobenzidine, as previously described (4). The number of vWF-stained vessels <100 μm in diameter per ×10 field were quantified and expressed as vessels per field. At least six nonoverlapping fields per animal were analyzed from three transverse sections obtained in nonbiased fashion from the left lung. Only fields consisting of alveolar septa were used; fields containing large vessels or conducting airways were avoided.

Determination of RV capillary density. RV capillary density was assessed using immunofluorescence microscopy after incubation of unstained RV sections with wheat germ agglutinin (WGA, a cell membrane marker) conjugated to Oregon Green 488 (Life Technologies, Grand Island, NY) and 4′-6-diamidino-2-phenylindole (DAPI, a nucleus marker; Life Technologies), as previously described (29). Capillaries were identified by autofluorescence surrounded by WGA staining. Capillaries and myocytes were manually counted in a blinded fashion to give a capillary-to-myocyte ratio per high-power field (×40 objective). At least three high-power fields per animal were analyzed.

Quantitative real-time RT-PCR. With the use of the Qiagen RNeasy Fibrous Tissue kit (QIAGEN Sciences, Germantown, MD), mRNA was carefully isolated from ~25 mg of homogenized RV tissue according to the manufacturer's protocol. RNA (1 μg) was reverse transcribed into complimentary DNA (cDNA) using a High-Capacity cDNA Reverse Transcription Kit (Applied Biosystems, Foster City, CA). cDNA was then diluted 10-fold, and real-time RT-PCR was performed using TaqMan Gene Expression Master Mix according to the manufacturer's instructions (Invitrogen Life Technologies, Carlsbad, CA). TaqMan Assay Primers included the following: α-myosin heavy chain (MHC) (*Myh6*; Rn00691721_g1), β-MHC (*Myh7*; Rn01488777_g1), and atrial natriuretic peptide (ANP) (*Nppa*; Rn00561661_m1); hypoxanthine phosphoribosyltransferase 1 was used as a housekeeping gene (*Hprt1*, Rn01527840_m1). All PCR reactions were performed using the Applied Biosystems 7500 Real-Time PCR System. Cycling parameters were as follows: 50°C for 2 min, 95°C for 10 min, and 95°C for 15 s followed by 60°C for 1 min for 40 cycles. *Hprt1* was used as the reference gene, and all gene expression results were expressed as mean fold change from controls ± SE.

Data and statistical analysis. Results are expressed as means ± SE. Where individual points are shown, results represent individual animals with horizontal lines depicting means and error bars representing SE. Experimental groups were compared by one-way ANOVA, using Tukey's multiple-comparison posttest analysis to determine between group differences (GraphPad Prism 5; GraphPad, La Jolla, CA). Grouped data sets were analyzed with two-way ANOVA. Differences at α-level of 0.05 ($P < 0.05$) were considered statistically significant.

RESULTS

Postnatal hyperoxia worsens PH in adulthood. We first evaluated the effects of hyperoxia and hypoxia on RVSP. Whereas brief (4-day) hyperoxia exposure alone did not alter RVSP, animals exposed to prolonged (10-day) hyperoxia had evidence of persistent PH at 12 wk of age (Fig. 2*A*). However, these elevations in RVSP were not as robust as those induced by chronic hypoxia exposure (Fig. 2*A*). As we hypothesized, hypoxia-induced increases in RVSP were most pronounced in animals exposed to postnatal hyperoxia. Whereas RVSP trended higher in $4d_{O_2}$-H vs. RA-H, it reached statistical significance in the $10dO_2$-H vs. RA-H group (Fig. 2*A*), indicating that postnatal hyperoxia exposure potentiates pulmonary hypertensive responses later in life by more than 30%.

We next evaluated the two-hit effects on RVH, as an established parameter reflecting changes in PA pressure and PA remodeling (45). Rats exposed to either brief or prolonged postnatal hyperoxia alone had no evidence of RVH (Fig. 2*B*). Following adult hypoxia exposure, all animals developed RVH consistent with a robust hypoxic PH phenotype (Fig. 2*B*). Importantly, both 4-day and 10-day hyperoxia exposure followed by adult hypoxia were associated with exaggerated RVH, suggesting that postnatal hyperoxia exposure alters RV responses to chronic hypoxia later in life. LV mass (expressed as LV + S weight indexed to body weight) was not affected by hyperoxia or hypoxia alone compared with RA controls (Fig. 2*C*). Interestingly, there was a significant increase in LV mass among animals exposed to 10 days of postnatal hyperoxia followed by adult hypoxia (Fig. 2*C*). Whereas postnatal hyperoxia did not significantly affect systemic pressures later in life, hypoxia exposure was associated with an increase in MAP, independent of early hyperoxia exposure (Fig. 2*D*). Taken together, these data suggest that postnatal hyperoxia exposure is associated with development of more severe PH upon hypoxia exposure later in life.

Postnatal hyperoxia-induced effects on PA pressures are not associated with increased vascular remodeling in the lung. We hypothesized that the increase in RVSP in the prolonged hyperoxia model was attributable to either elevated pulmonary vascular resistance created by hypoxia-induced PA remodeling with increased muscularization or to rarefaction of pulmonary microvessels as a direct result of the early hyperoxia exposure. As such, we analyzed the degree of small- and medium-sized PA muscularization as a function of PA wall area. As expected, all animals exposed to adult hypoxia developed increased PA muscularization, consistent with a hypoxic PH phenotype (Fig. 3*A*). However, there was no additive effect of postnatal hyperoxia on the degree of PA muscularization to account for the significant increases in RVSP among this group.

To assess for loss of pulmonary microvasculature, we analyzed the microvascular density per high-power field. Animals exposed to prolonged neonatal hyperoxia had a small but statistically significant decrease in pulmonary microvessel density (Fig. 3*B*). However, pulmonary microvessel rarefaction was not exacerbated further by postnatal hypoxia exposure, and no significant differences were seen between RA-H, $4dO_2$-H, or $10dO_2$-H animals. Furthermore, we did not find a significant increase in perivascular accumulation of inflammatory cells in any of the hypoxia-exposed groups, nor did we find any evidence of neointima formation or thrombotic occlu-

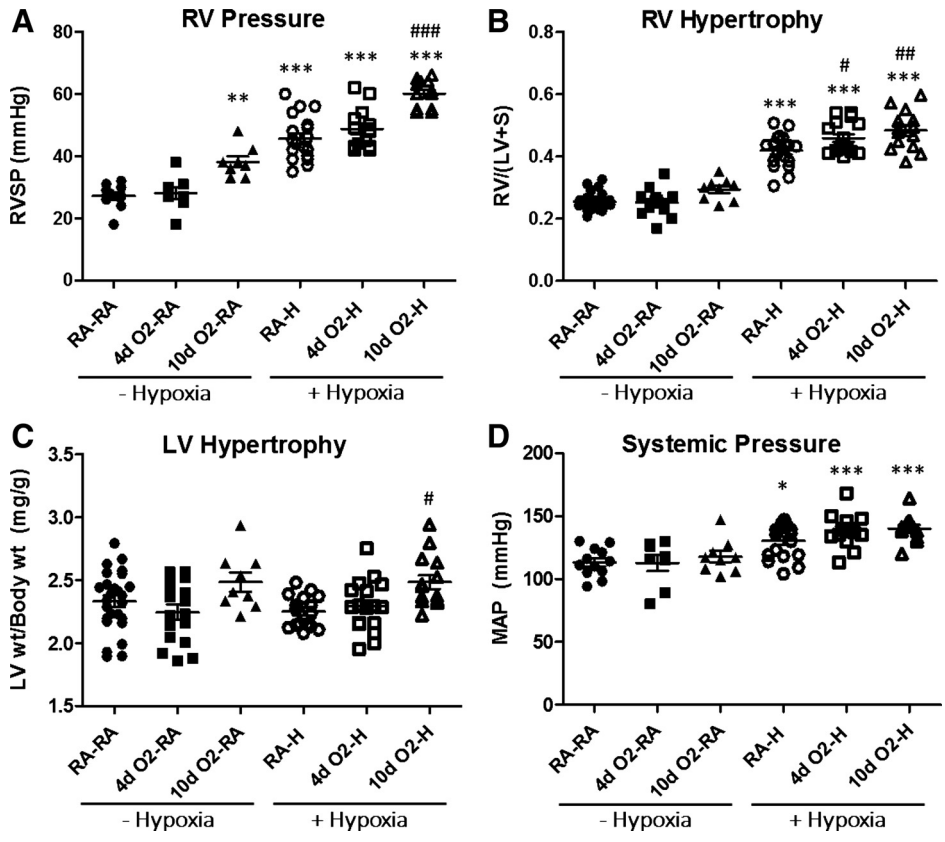

Fig. 2. Postnatal hyperoxia exposure leads to increased right ventricular systolic pressure (RVSP) and increased RV hypertrophy (RVH) after adult hypoxia exposure. Postnatal hyperoxia ($FI_{O_2} > 0.9$) exposure occurred for the first 4 or 10 days of life, respectively. Hypoxia exposure (P_{atm} = 362 mmHg for 2 wk) occurred from *week 10* to *week 12*. All end points were measured at 12 wk. *A*: pulmonary hypertension (PH) assessed by measurement of RVSP. PH develops after hypoxia exposure but is most severe in animals exposed to prolonged (10-day) postnatal hyperoxia. *B*: RVH assessment by Fulton index [weight of RV divided by weight of the left ventricle plus septum; RV/(LV + S)] following postnatal hyperoxia and adult hypoxia exposures. Note exaggerated RVH in animals exposed to postnatal hyperoxia and hypoxia. *C*: assessment of LV hypertrophy (reported as LV weight indexed to body weight) demonstrates similar LV hypertrophy among groups. *D*: mean arterial pressures (MAP) increase following hypoxia exposure but are not affected by hyperoxia exposure. Group labels are as outlined in Fig. 1. Points represent individual animals, and error bars represent means ± SE. Analysis by 1-way ANOVA; $*P < 0.05$, $**P < 0.01$, $***P < 0.001$ compared with RA control (RA-RA); $\#P < 0.05$, $\#\#P < 0.01$, $\#\#\#P < 0.001$ compared with RA-hypoxia (RA-H).

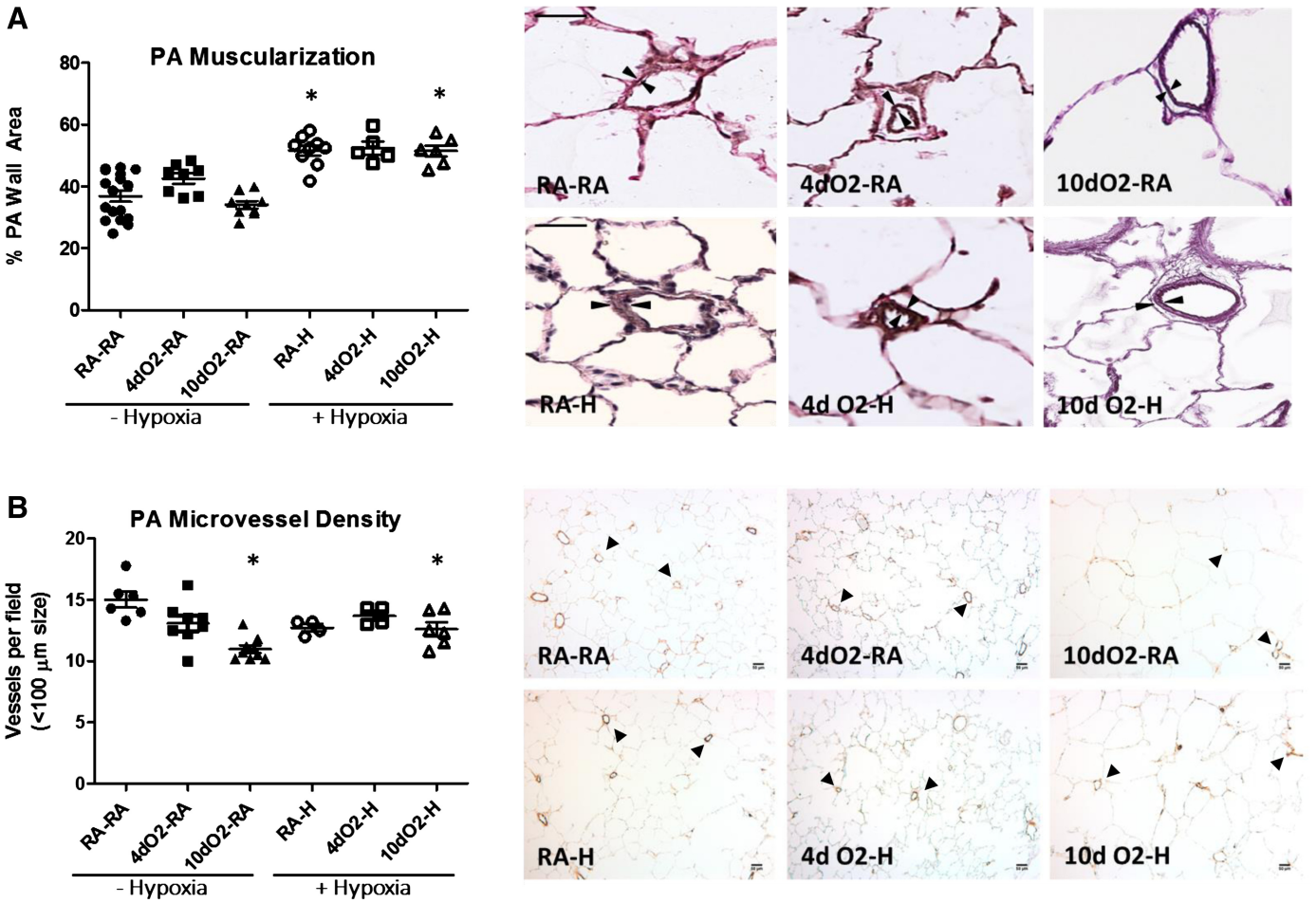

Fig. 3. Increased RVSP and increased RV hypertrophy in hyperoxia-hypoxia groups cannot be explained by increased pulmonary artery (PA) muscularization or decreased vascular density. *A*: Verhoff-van Gieson staining of lung demonstrates increased PA muscularization following hypoxia exposure with no additional effect of postnatal hyperoxia. PA muscularization was determined in a blinded fashion by dividing the measured pulmonary wall area by the entire vessel area. Representative images taken at ×20. Size bars = 50 μm. Note hypoxia-induced increase in PA wall thickness (indicated by arrowheads). *B*: von Willebrand factor staining demonstrates decreased pulmonary vascular density following hypoxia exposure (vessels marked by arrowheads). Note that animals exposed to prolonged neonatal hyperoxia had a small but statistically significant decrease in pulmonary microvessel density although pulmonary microvessel rarefaction was not exacerbated further by postnatal hypoxia exposure. Representative images taken at ×10. Size bars = 50 μm. Points represent individual animals, and error bars represent means ± SE. Analysis by 1-way ANOVA. *$P < 0.05$ compared with RA-RA.

sive disease to account for the significant increases in RVSP (data not shown). Thus the underlying mechanism of the increased PA pressures in postnatal hyperoxia-exposed animals may only be partially explained by increased rarefaction of pulmonary microvessels resulting from the initial hyperoxic exposure.

Postnatal hyperoxia is associated with more preserved RV function and exercise capacity following adult hypoxia exposure. To assess RV adaptation to the increased pulmonary vascular pressures, we measured CO via echocardiography. Intriguingly, both short (4 days) and especially prolonged (10 days) postnatal hyperoxia led to more preserved average CO following adult hypoxia compared with RA-H animals (Fig. 4*A*). Although there was a significant degree of heterogeneity in the 10dO$_2$-H group, this suggests better overall RV adaptation to adult hypoxia exposure following early hyperoxia. The increase in CO was driven entirely by increases in SV, as HR remained similar between groups (data not shown). To corroborate these data indicating increased CO in the 10dO$_2$-H group, we measured RV fractional shortening as a marker of RV contractility in a subset of RA-H and 10dO$_2$-H (32). As expected, the 10dO$_2$-H animals exhibited a significant increase in fractional shortening compared with RA-H animals, again indicating preserved cardiac function in this group (Fig. 4*B*).

To further evaluate the functional effects of these findings, we performed exercise testing, demonstrating preserved exercise capacity after hypoxia exposure in 10dO$_2$-H animals, whereas the RA-H and 4dO$_2$-H animals exhibited an expected decline in $\dot{V}O_{2\,max}$ after hypoxia exposure (Fig. 4*C*). Pre- and posthypoxia exposure weights were similar among all groups. Together, these data suggest a more adaptive RV phenotype following prolonged postnatal hyperoxia exposure.

Postnatal hyperoxia is associated with a more adapted RV phenotype. On the basis of our findings of more preserved RV function and exercise capacity in the 10dO$_2$-H group, we next sought to determine morphological and molecular correlates consistent with increased RV adaptation. Because of the lack of RV functional changes in the postnatal hyperoxia alone groups (Fig. 4), we focused these investigations on the hyperoxia-hypoxia-exposed groups. Because increases in RV capil-

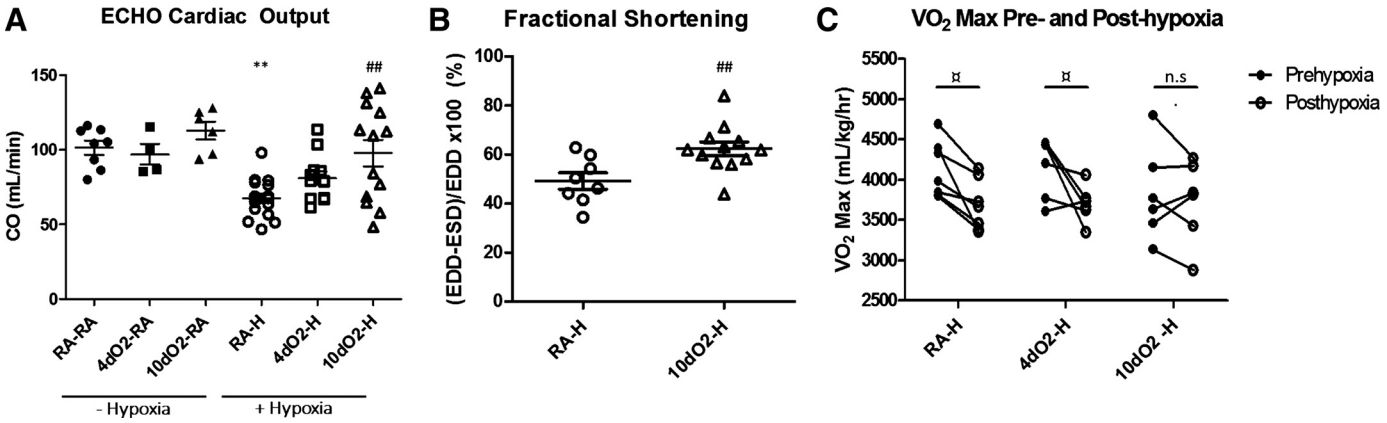

Fig. 4. Postnatal hyperoxia is associated with more preserved RV function and exercise capacity upon hypoxia exposure. *A*: cardiac output (CO) measured by echocardiography (ECHO) demonstrates cardiac dysfunction following hypoxia, with relative preservation of CO in animals exposed to prolonged postnatal hyperoxia. *B*: factional shortening, measured by the change in end-diastolic to end-systolic diameter over the end-diastolic diameter [(EDD − ESD)/EDD], was measured in a subset of hypoxia-exposed animals, again demonstrating significantly improved cardiac function in 10dO_2-H animals compared with RA-H. *C*: maximal exercise capacity declines as expected after adult hypoxia exposure, yet animals with prolonged postnatal hyperoxia exposure demonstrate no significant decrease in exercise capacity following adult hypoxia. Points represent individual animals, and error bars represent means ± SE. Analysis by 1-way ANOVA; $^{**}P < 0.01$ compared with RA-RA; $\#\#P < 0.01$ compared with RA-H; ¤$P < 0.05$ for pre- and posthypoxia comparison.

lary density have previously been shown to correlate with improved RV adaptation and function, we first evaluated this parameter (42). Indeed, the RV capillary density, expressed as a ratio of capillaries to myocytes per high-power field, was increased in animals exposed to postnatal hyperoxia, being especially pronounced in the 4dO_2-H group, which had an almost 50% increase in capillarization compared with RA controls (Fig. 5).

We next evaluated whether postnatal hyperoxia exposure results in a magnified switch back to a fetal gene profile in the RV, which could serve as a potential adaptive mechanism to better withstand hypoxic events (38, 40, 48). Reversion to a

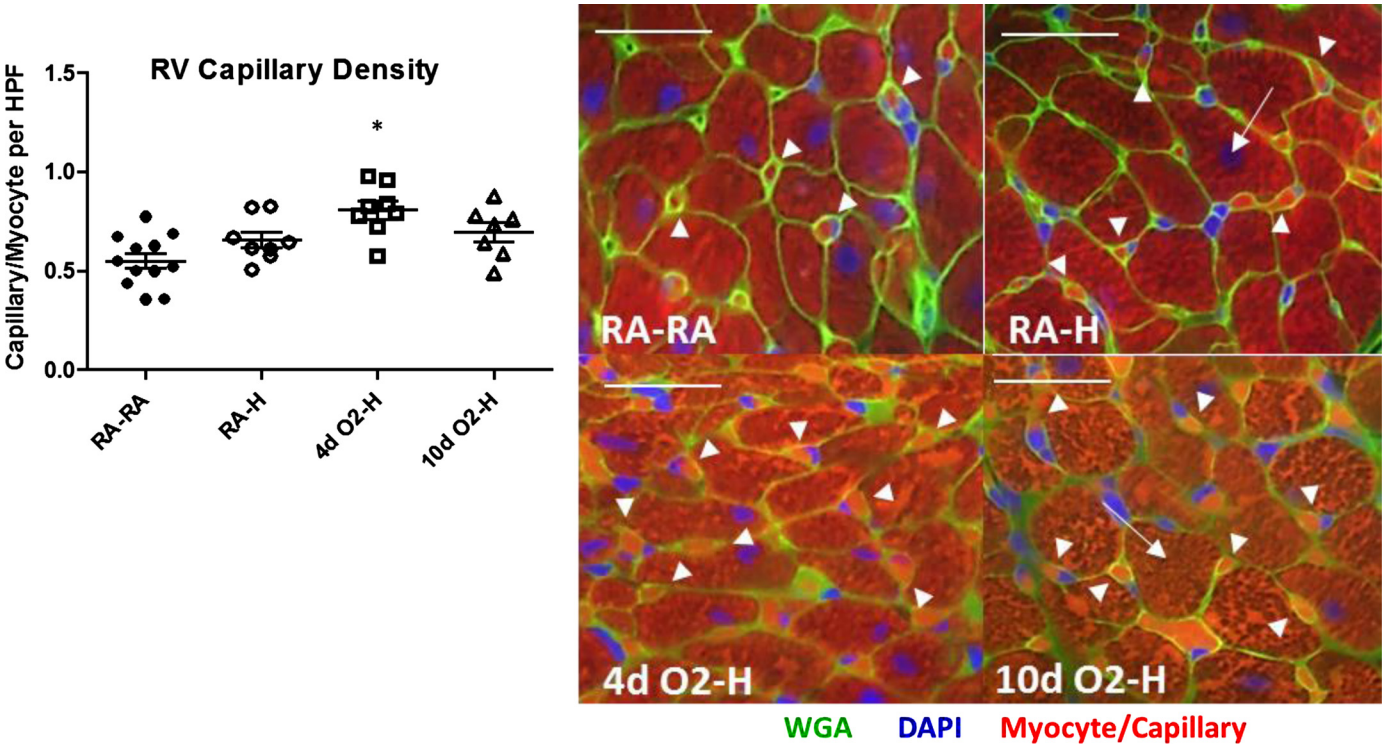

Fig. 5. Postnatal hyperoxia is associated with increased RV capillary density. RV capillary density was assessed by immunofluorescence. Wheat germ agglutinin (WGA) antibody was used to stain cell membranes (green), whereas nuclei were stained with 4′-6-diamidino-2-phenylindole (DAPI) (blue). Cardiomyocytes are identified by typical shape and myoglobin autofluorescence surrounded by WGA staining (arrows); capillaries are identified by size and autofluorescence surrounded by WGA staining (arrowheads). Cardiomyocytes and capillaries were quantified in a blinded fashion, and capillary-to-myocyte ratios were determined. *Left*: capillary/myocyte ratios after analysis. *Right*: representative images at ×40. Note increased capillarization following brief hyperoxia-hypoxia exposure. Size bars = 25 μm. Points represent individual animals, and error bars represent means ± SE. Analysis by 1-way ANOVA. $^{*}P < 0.05$ compared with RA-RA. HPF, high-power field.

fetal gene profile is well described in other models of PH and is associated with improved RV adaptation to afterload stress (40). This gene profile is characterized by decreased α-MHC expression and increased expression of β-MHC and ANP (33, 36, 48), a signature recapitulated in the RV of all animals exposed to adult hypoxia (Fig. 6, *A* and *B*). Of these, the expression levels of ANP were significantly augmented in hypoxic animals exposed to postnatal hyperoxia (Fig. 6*C*), suggesting an exaggerated shift to a fetal phenotype. Taken together, the data in Figs. 5 and 6 suggest a more adapted RV phenotype in hypoxic rats previously exposed to postnatal hyperoxia.

DISCUSSION

This study represents one of the most extensive functional evaluations examining the role of postnatal hyperoxia exposure in promoting adult PH, both independently and synergistically with adult hypoxia in a two-hit model of disease. We show that postnatal hyperoxia exaggerates pulmonary hypertensive responses upon hypoxia exposure later in life. Of note, these findings cannot be explained by exaggerated hypoxia-induced PA remodeling, neointimal formation, thrombotic lesions, or increased inflammatory deposits and are likely only partially explained by a decrease in lung vascular density. Interestingly, and somewhat unexpectedly, RV function and exercise capacity following hypoxia exposure were more preserved in the 10-day hyperoxia group, suggesting that prolonged postnatal hyperoxia exposure is associated with a more adaptive RV phenotype following hypoxia challenge later in life. Indeed, the results of our concomitant investigations of biochemical and structural endpoints in the RV suggest that postnatal hyperoxia is associated with a more adaptive RV phenotype to late pulmonary vascular insults.

In this rat model, brief hyperoxia alone did not result in late RVH or PH, whereas prolonged hyperoxia caused mild PH in adulthood (albeit without significant RVH). However, when combined with late hypoxia exposure, both brief and prolonged hyperoxia exposure caused robust RVH, but only prolonged hyperoxia significantly augmented RVSP. These findings indicate potentially differential effects of early hyperoxia exposure on the RV vs. the pulmonary vasculature.

The cause of the elevated RVSP in the animals exposed to prolonged hyperoxia may be partially explained by increased pulmonary resistance resulting from decreased pulmonary microvascular density. Previous studies have shown a decrease in pulmonary vascular density both in the immediate postnatal period and in the adult lung following postnatal hyperoxia exposure (6, 28, 49, 50, 57). Importantly, these effects are likely dependent on the duration and severity of hyperoxia exposure as well as the time point at which the pulmonary vascular density is evaluated (55). It is also possible that the elevations in RVSP in the prolonged hyperoxia-hypoxia group are the result of increased hypoxic pulmonary vasoconstriction although this was not assessed in this study and represents a potential area for future investigation. Such a potential for increased susceptibility to hypoxic pulmonary vasoconstriction is suggested by a study of adult subjects with a history of persistent PH of the newborn, who demonstrated a significant increase in RVSP by echocardiography at altitude compared with normal age-matched controls (41). It is also possible, given the improved CO noted by echocardiography, that the increased PA pressures in the hyperoxia-hypoxia group are a reflection of improved cardiac contractility and SV (12). Ongoing studies investigating hypoxic pulmonary vasoconstriction, cardiac contractility, and measures of PA-RV coupling in our model will be able to dissect the relative contribution of these factors.

Importantly, our data reinforce the notion that the presence of RVH alone is insufficient to discern between an adaptive vs. maladaptive cardiac response. By including physiological parameters in our assessment, we came to the surprising conclusion that postnatal hyperoxia exposure was associated with preserved CO and exercise capacity following hypoxia. This suggests that early hyperoxia exposure may have a priming effect on the RV, altering the RV compensatory response to later pulmonary vascular insults such as hypoxia. Cardiac preconditioning effects are well described in ischemia reperfusion models, but these effects typically last only 3 to 4 days at most (44, 58). Such long-term priming from postnatal events has not previously been described but may be most reminiscent of an Eisenmenger's phenomenon. In Eisenmenger's syndrome, CO is maintained despite severe elevations in pulmo-

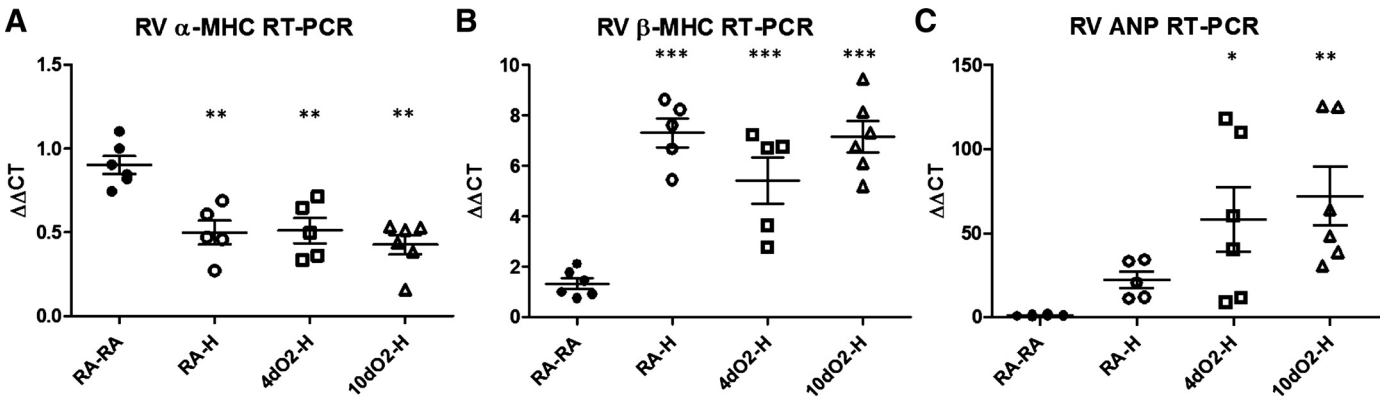

Fig. 6. Postnatal hyperoxia is associated with a more robust fetal gene expression pattern. End points were determined by real-time RT-PCR of RV homogenates. Hypoxia induces a decrease in α-myosin heavy chain (α-MHC, *A*) and increase in β-MHC (*B*) gene expression consistent with a fetal gene profile. Atrial natriuretic peptide (ANP) gene expression also increases after hypoxia exposure consistent with a fetal gene profile and is potentiated in animals with a history of early hyperoxia exposure (*C*). Points represent individual animals, and error bars represent means ± SE. Analysis by 1-way ANOVA. $^{*}P < 0.05$, $^{**}P < 0.01$, $^{***}P < 0.001$ compared with RA-RA.

nary vascular resistance and pressure, believed to be secondary to a continuous physiological RV priming from birth (19, 23, 25). Unfortunately, the mechanisms by which Eisenmenger's hearts remodel and adapt remain to be elucidated. Our studies may thus prove to be beneficial in understanding the priming effect that occurs in the Eisenmenger's RV as well as during and after early hyperoxia exposure.

We hypothesized that an earlier or exaggerated switch to a fetal gene pattern, with its relative preference for a hypoxic environment, could promote improved tolerance of adult hypoxia and account for the preserved CO and $\dot{V}O_{2\,max}$. Although alterations in α-MHC and β-MHC gene expression were similar among all hypoxia-exposed animals, even minor degrees of isoform switching, which may have been undetected in our study, could significantly impact contractility and tolerance of hypoxia (22, 34). The additive increments in ANP expression induced in the two-hit model are nevertheless consistent with development of a magnified fetal gene expression in the RV and may suggest a role for increased neurohormonal activation in these animals. Overall, the exact mechanism of such adaptive responses is unclear and merits further investigation and corroboration in alternative PAH models, such as the Sugen-hypoxia model. One potential modifier of improved RV function in our model may be improved mitochondrial biogenesis, and studies of mitochondrial function are currently ongoing in our laboratory. Lastly, because $\dot{V}O_{2\,max}$ is also affected by skeletal muscle function, we are investigating effects of perinatal hyperoxia and hypoxia on skeletal muscle function.

A potential limitation of our study is that the detection of several end points may be improved with more sensitive techniques, such as stereological assessment of capillary density or the use of RV pressure-volume conductance catheters, to gain further insight into mechanisms of increased PA pressures in the two-hit model. In addition, potential influences of sex on our results cannot be ruled out; however, although we included both male and female animals in our studies, numbers were too small for robust investigations of sex differences. Nevertheless, the major strength of our model is that it allows for a detailed physiological investigation of the effects of varying durations of postnatal hyperoxia and tolerance of later pulmonary vascular injury in the form of adult hypoxia exposure. Importantly, this novel two-hit animal model demonstrates that postnatal hyperoxia alone can result in long-term increases in PA pressures, identifying a notable risk factor that may help identify new populations at risk for developing PH (5, 16). Furthermore, we have identified a new paradigm in which the RV can actually be primed by early hyperoxia exposure to better tolerate later pulmonary vascular insults.

There is significant potential for clinical application of our study findings. We have demonstrated a clear association between early hyperoxia exposure and later development of PH. Given the high prevalence of premature deliveries and the extremely high incidence of oxygen exposure in premature infants, this may suggest a need for increased screening for PH in adults with a history of extreme prematurity. One limitation is that our model is not specifically a model of prematurity and, therefore, does not account for the totality of effects hyperoxia has on the developing cardiopulmonary system (37). However, neonatal rats are born with a simple saccular lung similar to that of extremely preterm infants (27), and early exposure of the neonatal rodent lung to hyperoxia reliably inhibits alveolar septal and microvascular development to recapitulate the hallmarks of human BPD (1, 2, 51). Thus our model remains highly relevant to the neonatal condition. Importantly, if these patients truly have improved adaptive properties of the RV, development of PH may go undetected for longer periods of time. Interestingly, a recent study published by Lewandowski et al. (31) demonstrated that increasing severity of prematurity was associated with increasing RV mass and an increased risk for RV dysfunction. Unfortunately, this study did not address the severity of concomitant pulmonary vascular disease, which could be expected to have a significant effect on RV function. However, that study as well as ours underscores the need for increased recognition of pulmonary vascular dysfunction in adults with a history of prematurity.

In summary, we found that postnatal hyperoxia exposure induces adult PH and potentiates the pulmonary vascular response to hypoxia. We also identified a potential cardiac priming effect of early hyperoxia exposure, resulting in significant resiliency and improved RV tolerance of late hypoxia-induced pulmonary vascular insults. Importantly, given that RV function is what ultimately drives morbidity and mortality in pulmonary vascular disease, improvement in the ability of the RV to compensate for pulmonary insults is critical to survival (14, 21). Further identification of the mechanisms by which these RVs may compensate could allow for targeted and RV-specific therapies to improve compensatory mechanisms in pediatric and adult forms of PH.

ACKNOWLEDGMENTS

The authors acknowledge Jordan Wood, BS, and Rebecca Roper for expert technical assistance.

GRANTS

This work was funded in part by NIH-T32 5T32HL091816-05 (K. Goss), Indiana University Showalter Research Trust Fund Grant (S. Ahlfeld), and VA Merit 1I01BX002042-01A2 (T. Lahm). This project was supported by the Indiana University Health-Indiana University School of Medicine Strategic Research Initiative.

DISCLOSURES

No conflicts of interest, financial or otherwise, are declared by the authors.

AUTHOR CONTRIBUTIONS

Author contributions: K.N.G., I.P., R.S.T., S.K.A., and T.L. conception and design of research; K.N.G., A.R.C., A.J.F., M.A., A.L.F., R.T., Y.G., M.B.B., and S.K.A. performed experiments; K.N.G., S.K.A., and T.L. analyzed data; K.N.G., M.B.B., R.S.T., S.K.A., and T.L. interpreted results of experiments; K.N.G. prepared figures; K.N.G. drafted manuscript; K.N.G., M.A., A.L.F., I.P., R.S.T., S.K.A., and T.L. edited and revised manuscript; K.N.G., A.R.C., A.J.F., M.A., A.L.F., R.T., Y.G., M.B.B., I.P., R.S.T., S.K.A., and T.L. approved final version of manuscript.

REFERENCES

1. **Ahlfeld SK, Conway SJ.** Aberrant signaling pathways of the lung mesenchyme and their contributions to the pathogenesis of bronchopulmonary dysplasia. *Birth Defects Res A Clin Mol Teratol* 94: 3–15, 2012.
2. **Ahlfeld SK, Conway SJ.** Assessment of inhibited alveolar-capillary membrane structural development and function in bronchopulmonary dysplasia. *Birth Defects Res A Clin Mol Teratol* 100: 168–179, 2014.
3. **Ahlfeld SK, Gao Y, Wang J, Horgusluoglu E, Bolanis E, Clapp DW, Conway SJ.** Periostin downregulation is an early marker of inhibited neonatal murine lung alveolar septation. *Birth Defects Res A Clin Mol Teratol* 97: 373–385, 2013.

4. **Aldred MA, Morrell NW.** Waiting in anticipation: the genetics of pulmonary arterial hypertension. *Am J Respir Crit Care Med* 186: 820–821, 2012.
5. **Austin ED, Kawut SM, Gladwin MT, Abman SH.** Pulmonary hypertension: NHLBI Workshop on the Primary Prevention of Chronic Lung Diseases. *Ann Am Thorac Soc* 11, *Suppl* 3: S178–S185, 2014.
6. **Balasubramaniam V, Mervis CF, Maxey AM, Markham NE, Abman SH.** Hyperoxia reduces bone marrow, circulating, and lung endothelial progenitor cells in the developing lung: implications for the pathogenesis of bronchopulmonary dysplasia. *Am J Physiol Lung Cell Mol Physiol* 292: L1073–L1084, 2007.
7. **Bates ML, Farrell ET, Eldridge MW.** Abnormal ventilatory responses in adults born prematurely. *N Engl J Med* 370: 584–585, 2014.
8. **Bedford TG, Tipton CM, Wilson NC, Oppliger RA, Gisolfi CV.** Maximum oxygen consumption of rats and its changes with various experimental procedures. *J Appl Physiol Respir Environ Exercise Physiol* 47: 1278–1283, 1979.
9. **Bhat R, Salas AA, Foster C, Carlo WA, Ambalavanan N.** Prospective analysis of pulmonary hypertension in extremely low birth weight infants. *Pediatrics* 129: e682–e689, 2012.
10. **Bhatt AJ, Pryhuber GS, Huyck H, Watkins RH, Metlay LA, Maniscalco WM.** Disrupted pulmonary vasculature and decreased vascular endothelial growth factor, Flt-1, and TIE-2 in human infants dying with bronchopulmonary dysplasia. *Am J Respir Crit Care Med* 164: 1971–1980, 2001.
11. **Bogaard HJ, Al Husseini A, Farkas L, Farkas D, Gomez-Arroyo J, Abbate A, Voelkel NF.** Severe pulmonary hypertension: The role of metabolic and endocrine disorders. *Pulm Circ* 2: 148–154, 2012.
12. **Champion HC, Michelakis ED, Hassoun PM.** Comprehensive invasive and noninvasive approach to the right ventricle-pulmonary circulation unit: state of the art and clinical and research implications. *Circulation* 120: 992–1007, 2009.
13. **Coalson JJ.** Pathology of bronchopulmonary dysplasia. *Semin Perinatol* 30: 179–184, 2006.
14. **D'Alonzo GE, Barst RJ, Ayres SM, Bergofsky EH, Brundage BH, Detre KM, Fishman AP, Goldring RM, Groves BM, Kernis JT, Levy PS, Pietra GG, Reid LM, Reeves JT, Rich S, Vreim CE, Williams GW, Wu M.** Survival in patients with primary pulmonary hypertension Results from a national prospective registry. *Ann Intern Med* 115: 343–349, 1991.
15. **Dauger S, Ferkdadji L, Saumon G, Vardon G, Peuchmaur M, Gaultier C, Gallego J.** Neonatal exposure to 65% oxygen durably impairs lung architecture and breathing pattern in adult mice. *Chest* 123: 530–538, 2003.
16. **Dweik RA, Rounds S, Erzurum SC, Archer S, Fagan K, Hassoun PM, Hill NS, Humbert M, Kawut SM, Krowka M, Michelakis E, Morrell NW, Stenmark K, Tuder RM, Newman J.** An official American Thoracic Society Statement: pulmonary hypertension phenotypes. *Am J Respir Crit Care Med* 189: 345–355, 2014.
17. **Erzurum S, Rounds SI, Stevens T, Aldred M, Aliotta J, Archer SL, Asosingh K, Balaban R, Bauer N, Bhattacharya J, Bogaard H, Choudhary G, Dorn GW 2nd, Dweik R, Fagan K, Fallon M, Finkel T, Geraci M, Gladwin MT, Hassoun PM, Humbert M, Kaminski N, Kawut SM, Loscalzo J, McDonald D, McMurtry IF, Newman J, Nicolls M, Rabinovitch M, Shizuru J, Oka M, Polgar P, Rodman D, Schumacker P, Stenmark K, Tuder R, Voelkel N, Sullivan E, Weinshilboum R, Yoder MC, Zhao Y, Gail D, Moore TM.** Strategic plan for lung vascular research: An NHLBI-ORDR Workshop Report. *Am J Respir Crit Care Med* 182: 1554–1562, 2010.
18. **Goldenberg RL, Culhane JF, Iams JD, Romero R.** Epidemiology and causes of preterm birth. *Lancet* 371: 75–84, 2008.
19. **Gomez-Arroyo J, Santos-Martinez LE, Aranda A, Pulido T, Beltran M, Muñoz-Castellanos L, Dominguez-Cano E, Sonnino C, Voelkel NF, Sandoval J.** Differences in right ventricular remodeling secondary to pressure overload in patients with pulmonary hypertension. *Am J Respir Crit Care Med* 189: 603–606, 2014.
20. **Harding R, Maritz G.** Maternal and fetal origins of lung disease in adulthood. *Semin Fetal Neonatal Med* 17: 67–72, 2012.
21. **Hemnes AR, Champion HC.** Right heart function and haemodynamics in pulmonary hypertension. *Int J Clin Pract Suppl* 11–19, 2008.
22. **Herron TJ, McDonald KS.** Small amounts of α-myosin heavy chain isoform expression significantly increase power output of rat cardiac myocyte fragments. *Circ Res* 90: 1150–1152, 2002.
23. **Hopkins WE, Ochoa LL, Richardson GW, Trulock EP.** Comparison of the hemodynamics and survival of adults with severe primary pulmonary hypertension or Eisenmenger syndrome. *J Heart Lung Transplant* 15: 100–105, 1996.
24. **Husain AN, Siddiqui NH, Stocker JT.** Pathology of arrested acinar development in postsurfactant bronchopulmonary dysplasia. *Hum Pathol* 29: 710–717, 1998.
25. **Kaemmerer H, Mebus S, Schulze-Neick I, Eicken A, Trindade PT, Hager A, Oechslin E, Niwa K, Lang I, Hess J.** The adult patient with Eisenmenger syndrome: a medical update after dana point part I: epidemiology, clinical aspects and diagnostic options. *Curr Cardiol Rev* 6: 343–355, 2010.
26. **Kallapur SG, Jobe AH.** Contribution of inflammation to lung injury and development. *Arch Dis Child Fetal Neonatal Ed* 91: F132–F135, 2006.
27. **Kimura J, Deutsch GH.** Key mechanisms of early lung development. *Pediatr Dev Pathol* 10: 335–347, 2007.
28. **Kunig AM, Balasubramaniam V, Markham NE, Morgan D, Montgomery G, Grover TR, Abman SH.** Recombinant human VEGF treatment enhances alveolarization after hyperoxic lung injury in neonatal rats. *Am J Physiol Lung Cell Mol Physiol* 289: L529–L535, 2005.
29. **Lahm T, Albrecht M, Fisher AJ, Selej M, Patel NG, Brown JA, Justice MJ, Brown MB, Van Demark M, Trulock KM, Dieudonne D, Reddy JG, Presson RG, Petrache I.** 17beta-Estradiol attenuates hypoxic pulmonary hypertension via estrogen receptor-mediated effects. *Am J Respir Crit Care Med* 185: 965–980, 2012.
30. **Lambert MI, Noakes TD.** Dissociation of changes in VO2 max, muscle QO2, and performance with training in rats. *J Appl Physiol* 66: 1620–1625, 1989.
31. **Lewandowski AJ, Bradlow WM, Augustine D, Davis EF, Francis J, Singhal A, Lucas A, Neubauer S, McCormick K, Leeson P.** Right ventricular systolic dysfunction in young adults born preterm. *Circulation* 128: 713–720, 2013.
32. **Lindqvist P, Henein M, Kazzam E.** Right ventricular outflow-tract fractional shortening: an applicable measure of right ventricular systolic function. *Eur J Echocardiogr* 4: 29–35, 2003.
33. **Lopaschuk GD, Jaswal JS.** Energy metabolic phenotype of the cardiomyocyte during development, differentiation, and postnatal maturation. *J Cardiovasc Pharm* 56: 130–140, 2010.
34. **Lowes BD, Minobe W, Abraham WT, Rizeq MN, Bohlmeyer TJ, Quaife RA, Roden RL, Dutcher DL, Robertson AD, Voelkel NF, Badesch DB, Groves BM, Gilbert EM, Bristow MR.** Changes in gene expression in the intact human heart. Downregulation of alpha-myosin heavy chain in hypertrophied, failing ventricular myocardium. *J Clin Invest* 100: 2315–2324, 1997.
35. **Madurga A, Mižíková I, Ruiz-Camp J, Morty RE.** Recent advances in late lung development and the pathogenesis of bronchopulmonary dysplasia. *Am J Physiol Lung Cell Mol Physiol* 305: L893–L905, 2013.
36. **Makinde AO, Kantor PF, Lopaschuk GD.** Maturation of fatty acid and carbohydrate metabolism in the newborn heart. *Mol Cell Biochem* 188: 49–56, 1998.
37. **O'Reilly M, Thébaud B.** Animal models of bronchopulmonary dysplasia: The term rat models. *Am J Physiol Lung Cell Mol Physiol* 307: L948–L958, 2014.
38. **Patterson AJ, Zhang L.** Hypoxia and fetal heart development. *Curr Mol Med* 10: 653–666, 2010.
39. **Prophet EB, Armed Forces Institute of Pathology.** *Laboratory Methods In Histotechnology*. Washington, DC: American Registry of Pathology, 1992.
40. **Rajabi M, Kassiotis C, Razeghi P, Taegtmeyer H.** Return to the fetal gene program protects the stressed heart: a strong hypothesis. *Heart Fail Rev* 12: 331–343, 2007.
41. **Sartori C, Allemann Y, Trueb L, Delabays A, Nicod P, Scherrer U.** Augmented vasoreactivity in adult life associated with perinatal vascular insult. *Lancet* 353: 2205–2207, 1999.
42. **Shiojima I, Sato K, Izumiya Y, Schiekofer S, Ito M, Liao R, Colucci WS, Walsh K.** Disruption of coordinated cardiac hypertrophy and angiogenesis contributes to the transition to heart failure. *J Clin Invest* 115: 2108–2118, 2005.
43. **Simonneau G, Gatzoulis MA, Adatia I, Celermajer D, Denton C, Ghofrani A, Gomez Sanchez MA, Krishna Kumar R, Landzberg M, Machado RF, Olschewski H, Robbins IM, Souza R.** Updated clinical classification of pulmonary hypertension. *J Am Coll Cardiol* 62: D34–D41, 2013.
44. **Stein AB, Tang XL, Guo Y, Xuan YT, Dawn B, Bolli R.** Delayed adaptation of the heart to stress: late preconditioning. *Stroke* 35: 2676–2679, 2004.

45. **Stenmark KR, Fagan KA, Frid MG.** Hypoxia-induced pulmonary vascular remodeling: cellular and molecular mechanisms. *Circ Res* 99: 675–691, 2006.
46. **Stenmark KR, Meyrick B, Galie N, Mooi WJ, McMurtry IF.** Animal models of pulmonary arterial hypertension: the hope for etiological discovery and pharmacological cure. *Am J Physiol Lung Cell Mol Physiol* 297: L1013–L1032, 2009.
47. **Stoll BJ, Hansen NI, Bell EF, Shankaran S, Laptook AR, Walsh MC, Hale EC, Newman NS, Schibler K, Carlo WA, Kennedy KA, Poindexter BB, Finer NN, Ehrenkranz RA, Duara S, Sanchez PJ, O'Shea TM, Goldberg RN, Van Meurs KP, Faix RG, Phelps DL, Frantz ID 3rd, Watterberg KL, Saha S, Das A, Higgins RD.** Neonatal outcomes of extremely preterm infants from the NICHD Neonatal Research Network. *Pediatrics* 126: 443–456, 2010.
48. **Taegtmeyer H, Sen S, Vela D.** Return to the fetal gene program: a suggested metabolic link to gene expression in the heart. *Ann NY Acad Sci* 1188: 191–198, 2010.
49. **Thebaud B, Abman SH.** Bronchopulmonary dysplasia: where have all the vessels gone? Roles of angiogenic growth factors in chronic lung disease. *Am J Respir Crit Care Med* 175: 978–985, 2007.
50. **Thibeault DW, Mabry S, Rezaiekhaligh M.** Neonatal pulmonary oxygen toxicity in the rat and lung changes with aging. *Pediatr Pulmonol* 9: 96–108, 1990.
51. **Thibeault DW, Mabry S, Rezaiekhaligh M.** Neonatal pulmonary oxygen toxicity in the rat and lung changes with aging. *Pediatr Pulmonol* 9: 96–108, 1990.
52. **Thibeault DW, Truog WE, Ekekezie II.** Acinar arterial changes with chronic lung disease of prematurity in the surfactant era. *Pediatr Pulmonol* 36: 482–489, 2003.
53. **Tishler PV, Larkin EK, Schluchter MD, Redline S.** Incidence of sleep-disordered breathing in an urban adult population: the relative importance of risk factors in the development of sleep-disordered breathing. *JAMA* 289: 2230–2237, 2003.
54. **Viscardi RM.** Perinatal inflammation and lung injury. *Semin Fetal Neonatal Med* 17: 30–35, 2012.
55. **Wang H, Jafri A, Martin RJ, Nnanabu J, Farver C, Prakash YS, MacFarlane PM.** Severity of neonatal hyperoxia determines structural and functional changes in developing mouse airway. *Am J Physiol Lung Cell Mol Physiol* 307: L295–L301, 2014.
56. **Wilson WL, Mullen M, Olley PM, Rabinovitch M.** Hyperoxia-induced pulmonary vascular and lung abnormalities in young rats and potential for recovery. *Pediatr Res* 19: 1059–1067, 1985.
57. **Yee M, White RJ, Awad HA, Bates WA, McGrath-Morrow SA, O'Reilly MA.** Neonatal hyperoxia causes pulmonary vascular disease and shortens life span in aging mice. *Am J Pathol* 178: 2601–2610, 2011.
58. **Yellon DM, Downey JM.** Preconditioning the myocardium: from cellular physiology to clinical cardiology. *Physiol Rev* 83: 1113–1151, 2003.